Dynamic tuning of an infrared hybrid-metamaterial resonance using vanadium dioxide

T. Driscoll,[1,a)] S. Palit,[2] M. M. Qazilbash,[1] M. Brehm,[3] F. Keilmann,[3] Byung-Gyu Chae,[4] Sun-Jin Yun,[4] Hyun-Tak Kim,[4] S. Y. Cho,[2] N. Marie Jokerst,[2] D. R. Smith,[1,2] and D. N. Basov[1]

[1]*Physics Department, University of California-San Diego, La Jolla, California 92093, USA*
[2]*Electrical and Computer Engineering Department, Duke University, P.O. Box 90291, Durham, North Carolina 27708, USA*
[3]*Abt. Molekulare Strukturbiologie, Max-Planck-Institut für Biochemie and Center for NanoScience, 82152 Martinsried, München, Germany*
[4]*IT Convergence & Components Lab, ETRI, Daejeon 305-350, Republic of Korea*

(Received 8 April 2008; accepted 2 June 2008; published online 14 July 2008)

We demonstrate a metamaterial device whose far-infrared resonance frequency can be dynamically tuned. Dynamic tuning should alleviate many bandwidth-related roadblocks to metamaterial application by granting a wide matrix of selectable electromagnetic properties. This tuning effect is achieved via a hybrid-metamaterial architecture; intertwining split ring resonator metamaterial elements with vanadium dioxide (VO_2)-a material whose optical properties can be strongly and quickly changed via external stimulus. This hybrid structure concept opens a fresh dimension in both exploring and exploiting the intriguing electromagnetic behavior of metamaterials. © *2008 American Institute of Physics*. [DOI: 10.1063/1.2956675]

Advances in the recently emerging field of metamaterials include the development and demonstration of devices for subwavelength imaging,[1] cloaking,[2] ultrafast optoelectric switching,[3] and more. So far, these devices have most often relied on geometrically fixed electromagnetic resonances which restrict operation to a single frequency[4,5] or narrow band.[6] Real-time tuning of the resonant response is one possible way to overcome limitations of bandwidth. Demonstrations of tuning have been made for microwave frequencies using integrated rf electrical components.[7] At infrared and higher frequencies, such components are unavailable, and other means of implementing tuning must be found.[8] Our hybrid split ring resonator vanadium dioxide (SRR-VO_2) device accomplishes this, granting a resonance tuning range of 20% or more.

Our device is made of 100 nm thick gold SRRs lithographically fabricated on a 90 nm layer of VO_2 [see Fig. 1(b)]. The VO_2 is grown on a sapphire substrate, and thoroughly characterized by electrical[9] and optical measurements.[10] VO_2 undergoes a thermally triggered insulator-to-metal phase transition[11] that corresponds to a four orders of magnitude change in conductivity. The SRR is the most common and best characterized implementation of electromagnetic metamaterials.[12–14] It responds resonantly to in-plane electric fields, and out-of-plane magnetic fields. The way which the VO_2 and SRR layers interact is what makes this hybid-metamaterial interesting. The thickness of the lithographic gold comprising the SRRs and of the VO_2 film are both much less than the in-plane periodicity of the SRR array (20 μm). Metamaterial arrays like this have been shown to form *effective* material layers whose electromagnetic thickness is approximately the period of the array,[14,15] rather than the physical thickness of the lithographic gold. In this arrangement, the local electromagnetic fields of the SRR overlap the VO_2 layer [see Fig. 1(c)] and intertwine with the VO_2 material response. The VO_2 film thus becomes part of this effective material layer—due to its proximity to the SRRs and thin size compared to the array periodicity. Together they form a hybrid metamaterial—blending the properties of the VO_2 film with those of the discrete SRR array.

The resonance frequency of the SRR metamaterial is highly sensitive to the dielectric property of any material placed nearby, especially in the vicinity of the SRR gaps.[16] This circumstance, along with the following distinctive dielectric property of VO_2, enables the realization of a dynamically tunable SRR-VO_2 hybrid metamaterial. Near its insulator-to-metal phase transition, VO_2 exhibits a divergent *bulk* permittivity [see Fig. 2(c)]. This modifies the local fields of the SRR within and around the gap region, acting like a tunable dielectric inside a capacitor. The resonance frequency of the SRR-VO_2 hybrid system is expected to decrease as VO_2 permittivity increases: a behavior anticipated from a simplified *RLC*-circuit model of SRR response. Ex-

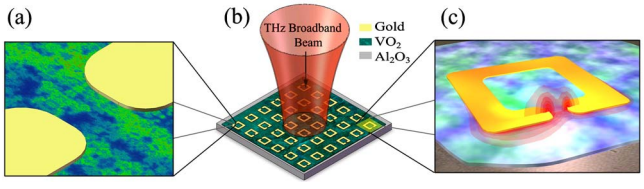

FIG. 1. (Color online) Sketch of the vanadium dioxide SRR hybrid-metamaterial. (a) Close-up of the SRR gap, sketched on top of a near-field image of a VO_2 film during phase transition. This comparison illustrates that the VO_2 percolating metallic grains (green) which emerge from the insulating host (blue) are much smaller than SRR gap. The sSNIM data is taken at 342 K. (b) Device layout and experimental setup. Gold SRRs of period 20 μm are lithographically fabricated above a 90 nm thick VO_2 layer, which has been grown on sapphire. The resonance of this hybrid-metamaterial device is probed in transmission. (c) Blow-up of a single SRR with electric field total amplitude results from a numerical solver, illustrating the overlap of the SRR fields with the VO_2 film.

[a)]Electronic mail: tdriscol@physics.ucsd.edu.

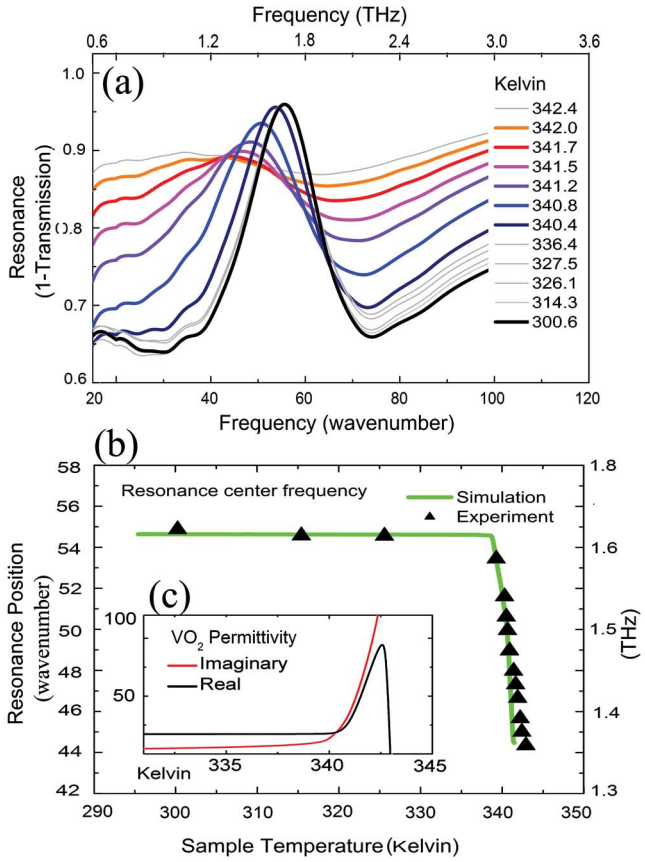

FIG. 2. (Color online) Dynamic tuning of the SRR w_0-resonance. (a) Transmission spectra through the hybrid metamaterial device at increasing sample temperatures. The resonance frequency decreases by nearly 20% as the vanadium dioxide passes through its metal insulator transition. (b) Resonance frequency as a function of temperature. (c) (inset in b) VO_2 Bruggeman effective-medium permittivity.

perimental results as well as numerical simulations, reported below, substantiate these expectations.

The observed divergent permittivity of the bulk VO_2 is understood to be due to the percolative nature of the phase transition. During its phase transition, VO_2 exhibits the emergence and growth of tiny (5–10 nm) metallic puddles [see Fig. 1(a)] in the insulating host. Figure 1(a) illustrates this, showing near-field composition data obtained via scattering scanning near-field infrared microscope (sSNIM), overlaid on a sketch of the 3 μm wide SRR gap. The *effective medium* response of the bulk VO_2 material comprised of these metal and insulating puddles is described by the Bruggeman model.[10] This arrangement is interesting as it utilizes one nanometer-scale effective-medium (formed by metallic puddles in the VO_2 insulation host) within another micron-size effective medium (formed by the periodic SRR array).

To probe this hybrid metamaterial, we perform Fourier transform infrared transmission spectroscopy of our device. We focus normally incident linearly polarized light from a mercury lamp onto a 3 mm^2 spot on the 1 cm^2 sample. The SRR array is oriented such as to electrically excite the SRR by taking advantage of the asymmetrical in-plane dipole moment created in the long and short legs of the SRR.[17,18] In Fig. 2, we display transmission spectra for our hybrid device. The room temperature spectra reveal a strong resonance with a peak at 55 cm^{-1} [see Fig. 2(a)]. As we increase the temperature of the device, VO_2 begins its transition and the observed resonance peak frequency decreases. The tuning of the resonance through the VO_2 transition can be mapped by plotting the peak frequency versus temperature [see Fig. 2(b)]. The resultant curve shows a sharp onset of tuning as the phase transition begins, and has a tuning range of 20%. At temperatures above 342 K, the resonance becomes heavily damped due to the increasing conductivity of the VO_2 layer. Eventually, the interconnecting VO_2 metallic puddles electrically short the SRR entirely, giving us the ability to turn the resonance off at temperatures above 343 K.

We substantiate our experimental observations numerically—simulating the metamaterial using the finite-integration time-domain code package Microwave Studio by CST, Inc. All three constituents of the device (SRR, VO_2, Al_2O_3 substrate) are included. These numerical results agree very well with our experimental data—showing a room temperature resonance at 55 cm^{-1}. Simulations for elevated temperatures [green tuning curve shown in Fig. 2(b)] use Bruggeman permittivity values for VO_2 taken from Fig. 2(c),[10] and also agree well with experimental data. The accuracy of Microwave Studio for the prediction of the resonance tuning of our SRR-VO_2 hybrid is important, since metamaterial design advances are largely reliant on such numerical simulators.

In order to evaluate the parameter space where this hybrid-metamaterial device enables tunable electromagnetic properties, we retrieve permittivity and permeability values for the metamaterial layer. This is done by modeling the transmission through a two-layer device (hybrid SRR+VO_2 and Al_2O_3 substrate) using the Fresnel equations. Electromagnetic oscillators are assigned to the material of each layer, and then fit to the observed spectra.[14] Literature values for the permittivity of Al_2O_3 are used for the substrate.[19] The oscillator used for the hybrid metamaterial layer is a modified Lorentzian—incorporating effects arising from the spatial dispersion present in the SRR array.[20] This recent advance in our fitting procedure gives a noticeable improvement in fit over previous oscillator models.[21] Figure 3 shows the retrieved real permittivity and permeability. The room temperature permittivity exhibits an expected strong resonance. Room temperature permeability also shows a weak antiresonance, even in our electric excitation configuration. This is an artifact of the SRR array periodicity; spatial dispersion acts to couple the permittivity resonance to a permeability antiresonance. This effect has been routinely observed for metamaterials with periodicity such as ours—in the range of one-tenth of a wavelength.[22]

At temperatures above 340 K, the retrieved permittivity and permeability resonances both redshift. This frequency shift follows the transition from insulator to metal with temperature in VO_2. Losses in the VO_2 metallic puddles also damp the resonance, decreasing the amplitude. Any nontunable metamaterial allows only a *single* pair of permittivity and permeability curves. In contrast, the shaded area in Fig. 3 illustrates a range of permittivity and permeability values accessible with the help of our hybrid SRR-VO_2 device. Through careful control of the sample temperature, we can select any permittivity-permeability curve pair in the shaded region. Electromagnetic flexibility of this kind is immensely valuable in device design and operation.

The accuracy of our oscillator-fitting model in replicating the observed experimental spectra highlights the essence

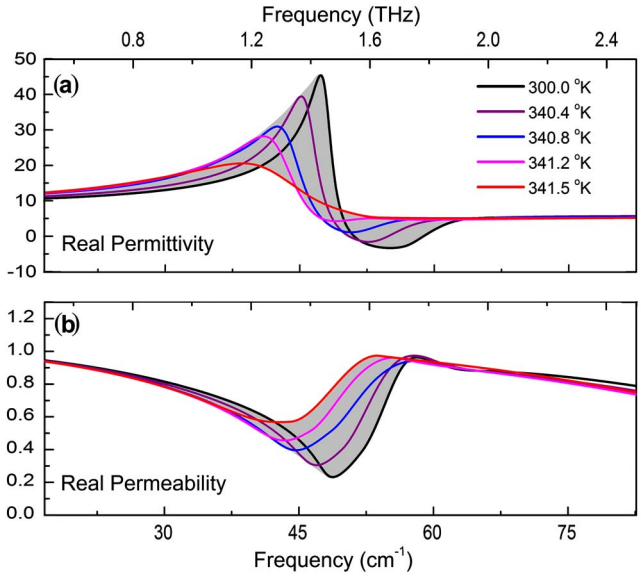

FIG. 3. (Color online) Experimentally retrieved permittivity and permeability bandwidth for the hybrid metamaterial. (a) Permittivity values for the SRR-VO_2 hybrid layer in our device. (b) Permeability values. The shaded area illustrates the complete range of values accessible with the help of our hybrid SRR-VO_2 device

of the hybrid-metamaterial approach. Physically, our gold SRR array and VO_2 film comprise two distinct layers, each only ~100 nm thick. Electromagnetically, however, these two layers are exceedingly well represented by one single hybrid-material layer with combined properties of SRR and VO_2. As mentioned, the electromagnetic thickness of a SRR array is approximated by the array periodicity, which can be quite large compared to the physical thickness of the SRR. It is this large electromagnetic thickness which allows us to easily combine the properties of other nearby materials with those of the metamaterial, forming a hybrid-metamaterial.

We stress that the phase transition in VO_2 may be triggered optically[23] or electrically[24] as well as thermally, thus enabling photonic or electric control of the resonance in this hybrid metamaterial. In these cases, one can envision locally triggered sections of VO_2 for pixel-like tuning of the metamaterial. Taking advantage of advanced device architectures can also expand the range of tuning, by making every attempt to maximize the SRR electric flux inside the VO_2. Simulations performed employing embedded SRRs in thicker 500 nm VO_2 reveal a resonance shift of up to 40%—twice the range of our demonstrated device. Our demonstration of dynamic tuning in this SRR-VO_2 configuration suggests the potential for rich physics and interesting effects in other hybrid-metamaterial devices employing magnetic, nonlinear, or other materials. Combining the wide ranging phenomena found in natural materials with the electromagnetic design control offered by metamaterials may act to expand the usefulness of each.

The authors are grateful for and wish to acknowledge funding for this project from AFOSR MURI (W911NF-04-1-0247), FA 9550-06-01-0279, and ETRI.

[1] J. B. Pendry, Phys. Rev. Lett. **85**, 18 (2000).
[2] J. B. Pendry, D. Schurig, and D. R. Smith, Science **312**, 1780 (2006).
[3] H.-T. Chen, W. J. Padilla, J. M. O. Zide, A. C. Gossard, A. J. Taylor, and R. D. Averitt, Nature (London) **444**, 597 (2006).
[4] D. Schurig, J. J. Mock, B. J. Justice, S. A. Cummer, J. B. Pendry, A. F. Starr, and D. R. Smith, Science **314**, 977 (2006).
[5] Z. Liu, H. Lee, Y. Xiong, C. Sun, and X. Zhang, Science **315**, 1686 (2007).
[6] T. Driscoll, D. N. Basov, A. F. Starr, P. M. Rye, S. Nemat-Nasser, D. Schurig, and D. R. Smith, Appl. Phys. Lett. **88**, 081101 (2006).
[7] I. V. Shadrivov, S. K. Morrison, and Y. S. Kivshar, Opt. Express **14**, 9344 (2006).
[8] H.-T. Chen, J. F. O'Hara, A. K. Azadi, A. J. Taylor, R. D. Averitt, D. B. Shrekenhamer, and W. J. Padilla, Nat. Photonics **2**, p. 295 (2008).
[9] Y. J. Chang, J. S. Yang, D. H. Kim, T. W. Noh, D. W. Kim, E. O. Kahng, B. Kahng, and J. S. Chung, Phys. Rev. B **76**, 075118 (2007).
[10] M. M. Qazilbash, M. Brehm, B.-G. Chae, P.-C. Ho, G. O. Andreev, B.-J. Kim, S. J. Yun, A. V. Balatsky, M. B. Maple, F. Keilmann, H.-T. Kim, and D. N. Basov, Science **318**, 1750 (2007).
[11] A. Zylbersztejn and N. F. Mott, Phys. Rev. B **11**, 4383 (1975).
[12] W. J. Padilla, D. N. Basov, and D. R. Smith, Mater. Today **9**, 28 (2006).
[13] D. R. Smith and J. B. Pendry, J. Biomed. Opt. **23**, 3 392 (2006).
[14] T. Driscoll, D. N. Basov, W. J. Padilla, J. J. Mock, and D. R. Smith, Phys. Rev. B **75**, 115114 (2007).
[15] D. R. Smith, D. Schurig, and J. J. Mock, Phys. Rev. E **74**, 036604 (2006).
[16] T. Driscoll, G. O. Andreev, D. N. Basov, S. Palit, S. Y. Cho, N. M. Jokerst, and D. R. Smith, Appl. Phys. Lett. **91**, 062511 (2007).
[17] W. J. Padilla, A. J. Taylor, C. Highstrete, M. Lee, and R. D. Averitt, Phys. Rev. Lett. **96**, 107401 (2006).
[18] N. Katsarakis, G. Konstantinidis, A. Kostopoulos, R. S. Penciu, T. F. Gundogdu, M. Kafesaki, E. N. Economou Th. Koschny, and C. M. Soukoulis, Opt. Lett. **30**, 1348 (2005).
[19] D. Billard, F. Gervais, and B. Piriou, Int. J. Infrared Millim. Waves **1**, 4 (1980).
[20] R. Liu, T. J. Cui, D. Huang, and B. Zhao, Phys. Rev. E **76**, 026606 (2007).
[21] T. Driscoll, G. O. Andreev, D. N. Basov, S. Palit, T. Ren, J. Mock, S.-Y. Cho, N. M. Jokerst, and D. R. Smith, Appl. Phys. Lett. **90**, 092508 (2007).
[22] T. Koschny, P. Markos, and D. R. Smith, Phys. Rev. E **68**, 065602 (2003).
[23] M. Rini, A. Cavalleri, R. W. Schoenlein, R. Lopez, L. C. Feldman, R. F. Haglund, L. A. Boatner, and T. E. Haynes, Opt. Lett. **30**, 1 (2004).
[24] H. T. Kim, B. G. Chae, D. H. Youn, S. L. Maeng, G. Kim, K. Y. Kang, and Y. S. Lim, New J. Phys. **6**, 52 (2004).

射 频 和 天 线 设 计 培 训 课 程 推 荐

易迪拓培训(www.edatop.com)由数名来自于研发第一线的资深工程师发起成立，致力并专注于微波、射频、天线设计研发人才的培养；我们于 2006 年整合合并微波 EDA 网(www.mweda.com)，现已发展成为国内最大的微波射频和天线设计人才培养基地，成功推出多套微波射频以及天线设计经典培训课程和 ADS、HFSS 等专业软件使用培训课程，广受客户好评；并先后与人民邮电出版社、电子工业出版社合作出版了多本专业图书，帮助数万名工程师提升了专业技术能力。客户遍布中兴通讯、研通高频、埃威航电、国人通信等多家国内知名公司，以及台湾工业技术研究院、永业科技、全一电子等多家台湾地区企业。

易迪拓培训课程列表：http://www.edatop.com/peixun/rfe/129.html

射频工程师养成培训课程套装

该套装精选了射频专业基础培训课程、射频仿真设计培训课程和射频电路测量培训课程三个类别共 30 门视频培训课程和 3 本图书教材；旨在引领学员全面学习一个射频工程师需要熟悉、理解和掌握的专业知识和研发设计能力。通过套装的学习，能够让学员完全达到和胜任一个合格的射频工程师的要求…

课程网址：http://www.edatop.com/peixun/rfe/110.html

ADS 学习培训课程套装

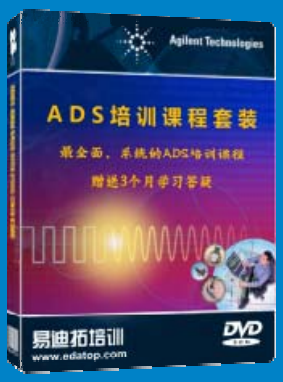

该套装是迄今国内最全面、最权威的 ADS 培训教程，共包含 10 门 ADS 学习培训课程。课程是由具有多年 ADS 使用经验的微波射频与通信系统设计领域资深专家讲解，并多结合设计实例，由浅入深、详细而又全面地讲解了 ADS 在微波射频电路设计、通信系统设计和电磁仿真设计方面的内容。能让您在最短的时间内学会使用 ADS，迅速提升个人技术能力，把 ADS 真正应用到实际研发工作中去，成为 ADS 设计专家...

课程网址： http://www.edatop.com/peixun/ads/13.html

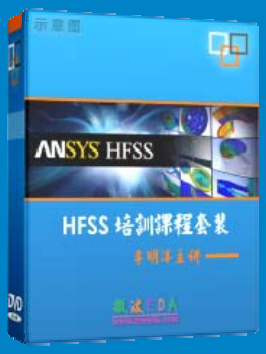

HFSS 学习培训课程套装

该套课程套装包含了本站全部 HFSS 培训课程，是迄今国内最全面、最专业的 HFSS 培训教程套装，可以帮助您从零开始，全面深入学习 HFSS 的各项功能和在多个方面的工程应用。购买套装，更可超值赠送 3 个月免费学习答疑，随时解答您学习过程中遇到的棘手问题，让您的 HFSS 学习更加轻松顺畅…

课程网址：http://www.edatop.com/peixun/hfss/11.html

CST 学习培训课程套装

该培训套装由易迪拓培训联合微波 EDA 网共同推出，是最全面、系统、专业的 CST 微波工作室培训课程套装，所有课程都由经验丰富的专家授课，视频教学，可以帮助您从零开始，全面系统地学习 CST 微波工作的各项功能及其在微波射频、天线设计等领域的设计应用。且购买该套装，还可超值赠送 3 个月免费学习答疑…

课程网址：http://www.edatop.com/peixun/cst/24.html

HFSS 天线设计培训课程套装

套装包含 6 门视频课程和 1 本图书，课程从基础讲起，内容由浅入深，理论介绍和实际操作讲解相结合，全面系统的讲解了 HFSS 天线设计的全过程。是国内最全面、最专业的 HFSS 天线设计课程，可以帮助您快速学习掌握如何使用 HFSS 设计天线，让天线设计不再难…

课程网址：http://www.edatop.com/peixun/hfss/122.html

13.56MHz NFC/RFID 线圈天线设计培训课程套装

套装包含 4 门视频培训课程，培训将 13.56MHz 线圈天线设计原理和仿真设计实践相结合，全面系统地讲解了 13.56MHz 线圈天线的工作原理、设计方法、设计考量以及使用 HFSS 和 CST 仿真分析线圈天线的具体操作，同时还介绍了 13.56MHz 线圈天线匹配电路的设计和调试。通过该套课程的学习，可以帮助您快速学习掌握 13.56MHz 线圈天线及其匹配电路的原理、设计和调试…

详情浏览：http://www.edatop.com/peixun/antenna/116.html

我们的课程优势：

※ 成立于 2004 年，10 多年丰富的行业经验，

※ 一直致力并专注于微波射频和天线设计工程师的培养，更了解该行业对人才的要求

※ 经验丰富的一线资深工程师讲授，结合实际工程案例，直观、实用、易学

联系我们：

※ 易迪拓培训官网：http://www.edatop.com

※ 微波 EDA 网：http://www.mweda.com

※ 官方淘宝店：http://shop36920890.taobao.com